A simple diffusion-controled model of mixing across a stable density interface

C. Kranenburg

VERVALLEN

Internal Report No. 2-79

Laboratory of Fluid Mechanics

Department of Civil Engineering

Delft University of Technology

A SIMPLE DIFFUSION-CONTROLED MODEL OF MIXING ACROSS A STABLE DENSITY INTERFACE

Internal Report No. 2-79

C. Kranenburg

Laboratory of Fluid Mechanics
Department of Civil Engineering
Delft University of Technology

1979

CONTENTS

Notation

a, A, b	constants
c	velocity of propagation
E	$= w_e/u_*$, dimensionless entrainment velocity
f	function of dimensionless pressure gradient
F_s, F_m	functions of gradient Richardson number to account for the damping of turbulence by density differences
g	gravitational constant
h	depth of mixed layer
k	turbulent kinetic energy
K, K_s	eddy diffusivity
K_m	eddy viscosity
l	length scale of large eddies
p	pressure
Re_*	$= hu_*/\nu_o$, Reynolds number
Rf	flux Richardson number, defined by equation 8
Ri	gradient Richardson number, defined by equation 6
Ri_*	$= \Delta\rho_o g h_o/(\rho_o u_*^2)$, overall Richardson number
t	time
u, v, w	horizontal, transverse and vertical velocity components
U	dimensionless horizontal velocity defined by equation 11b
w_e	entrainment velocity
x, z	spatial co-ordinates, the z-axis points downwards
y	$= ct-z$, co-ordinate in moving frame of reference
$\alpha, \alpha_s, \alpha_m$	constants
γ	$= h\, \partial\bar{p}/\partial x/(\rho_o u_*^2)$, dimensionless pressure gradient
Γ	scalar
Δu	difference between mean horizontal velocity of mixed layer and velocity just below the interface
$\Delta\rho$	$= \rho_o - \bar{\rho}(0,t)$, density difference between lower layer and free surface
η	$= z/h(t)$, dimensionless vertical co-ordinate
η_e	value of η where Rf/F_m is maximum
κ	von Kármán's constant

κ/κ_s	turbulent Prandtl number under neutral conditions
ν_o	molecular or effective viscosity just below interface
ρ	density
ρ_o	density of lower layer
P	dimensionless density difference defined by equation 11a
$\bar{..}$	mean value as regards turbulence
$..'$	turbulent fluctuation
$\bar{\bar{..}}$	depth averaged value

<u>subscripts</u>

cr	critical value
m	momentum
max	maximum value
n	neutral conditions
s	scalar
o	initial condition, lower layer
*	referring to friction velocity

Abstract

Mixing across a stable density interface caused by a shear stress externally acting on a two-layer fluid initially at rest is modelled using the turbulent-diffusion concept. The influence of a (relatively weak) longitudinal pressure gradient is also considered. The central point of view developed is that the mixed layer can be only weakly stratified so that the buoyancy transport across the mixed layer, and not the processes near the interface, controls the entrainment rate. To model the turbulent transports of buoyancy and momentum, common expressions for gradient transport in turbulent Couette and channel flow are adopted. Using a similarity solution, results are given for small and large Ri_*, where Ri_* is the overall Richardson number based on the friction velocity. The entrainment rate obtained does not depend on Ri_* at small Ri_*, and is inversely proportional to Ri_* at large Ri_*. The latter result is derived without introducing the usual assumption that the increase in potential energy is proportional to the work done by the shear stress, which assumption leads to the same result. An adverse pressure gradient is found to decrease the entrainment rate. An estimate of the mean velocity of the mixed layer is given.

1. Introduction

Two cases can be distinguished as regards turbulent mixing across a stable density interface. The turbulence can be generated internally, by a developing shear flow for instance, or externally at (one of) the boundaries of the flow field. The latter case is considered in this note. One well-known example of externally generated turbulence is the mixing in the upper layer and related deepening of the thermocline caused by wind blowing over a thermally stratified lake.

Figure 1 shows the situation to be examined. A two-layer system is initially at rest, both layers being constant-density layers. The fractional density difference is much less than unity, and transfer of heat or mass across the free surface is absent. At a certain instant a prescribed shear stress which afterwards remains constant starts to act at the free surface, and a (weak) longitudinal pressure gradient may be present. The resulting flow is assumed to be nearly homogeneous in the horizontal direction. The mean velocity gradients in the upper layer will cause turbulence, which in turn leads to 'erosion' of the density interface: fluid from the lower layer is transferred across the interface and is mixed within the upper layer while the interface remains sharp. The depth of the upper layer increases as time elapses. One question which can be asked is at what (entrainment) rate this depth increases.

This subject has intrigued numerous research-workers for some decades: reference is made here to the reviews by Turner (1), Long (2), and Sherman et al. (3). Among the laboratory experiments done, those of Kato and Phillips (4) are frequently quoted. The rates of entrainment these authors find seem to agree, at least so far as the order of magnitude is concerned, with measurements in nature (e.g. Ottesen Hansen (5), Kullenberg (6)). In particular, many investigations show the entrainment rate to be more or less inversely proportional to an overall Richardson number at sufficiently large values of this parameter.

Theoretical approaches have been based on (i) overall energy considerations, and (ii) higher-order turbulence models. The former method is somewhat intuitive, the crucial assumption being that the increase in potential energy owing to mixing is proportional to the work done by the shear stress. Higher order turbulence models involve a complicated set of equations which must be solved numerically.

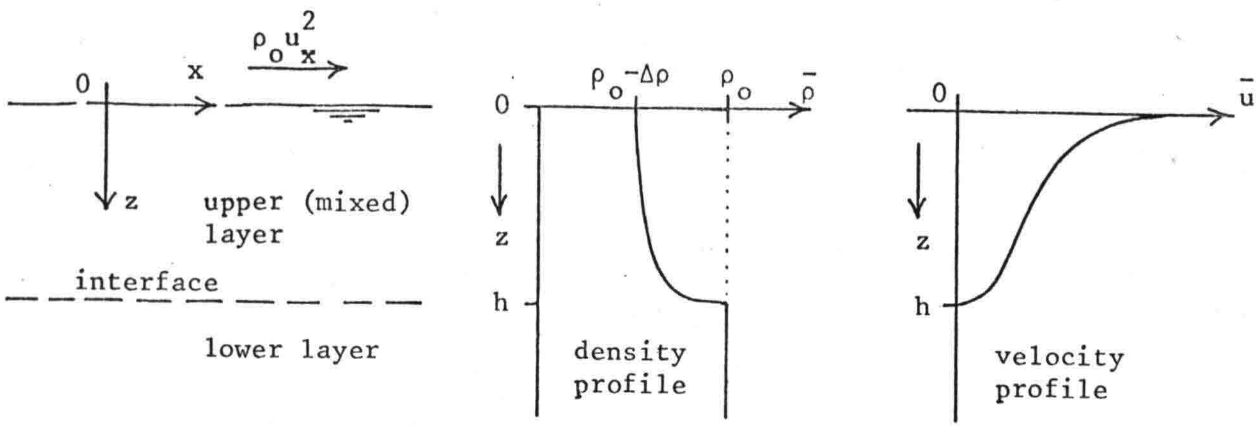

Figure 1. Diagram of case considered

The aim of the present note is to establish a possible constraint on the rate of entrainment imposed by the turbulence in the upper layer and to tentatively find out what kind of turbulence modelling would be required to predict realistic entrainment rates. Furthermore, the influence of a longitudinal pressure gradient on entrainment is examined. Some semi-quantitative results are obtained using the gradient-transport concept. Secondary flows, such as Langmuir circulations, are not considered explicitly.

2. Physical startingpoints

The object of the following observations is to provide a basis for the analytical development presented in section 3.

- The interface remains sharp as it moves downwards, and the fluid in the lower layer is not, or relatively little, disturbed. As such the process has a wave-like character: the interface can be conceived of as the front of a kinematic wave. It is therefore not obvious beforehand to model entrainment as a diffusion process. However, if the diffusive properties of the fluid depend on the distance to the front in a certain way, the diffusion process will have a wave-like character. This point is discussed further in the Appendix.
- The buoyancy transport in the mixed (upper) layer suppresses the turbulence, and, correspondingly, the vertical transport capacity. For given shear stress at the free surface and longitudinal pressure gradient there will therefore exist an upper limit to the buoyancy flux. Measurements (4, 7, 12, 22) indicate that the mean velocity gradients are extreme near the free surface and the interface. Therefore, the turbulence will be suppressed most effectively at an intermediate level. See sections 3.1 and 3.4 for a further discussion.

- If the flow in the upper layer would be laminar, entrainment would not occur (8). It is therefore the turbulence, and not the mean flow, that causes the erosion ('detachment of whisps of fluid', (4)) of the interface. This indicates that the turbulence near the interface can be only slightly (or not) inhibited by buoyancy effects, and that the local Richardson numbers are small. An eroded (or thinned) interface is unstable, and Kelvin-Helmholtz instability would cause breaking of internal waves (8, 10). The analysis of Hazel (9), for instance, indicates that at small Richardson numbers the growth rates of unstable waves are more or less inversely proportional to the thickness of the interface. The growth of unstable waves would therefore always become a rapid process at an interface which is continuously eroded. As a consequence, the mixing in the upper layer becomes the controling process, and wave breaking occurs only after the mixing has proceeded to a certain degree. The breaking of waves will therefore take place intermittently.

The basic assumption here is that the rate of entrainment is determined by the vertical transport capacity of the mixed layer, and that the wave breaking and mixing at the interface is sufficiently rapid to provide the buoyancy flux the mixed layer is able to transport (this presupposes miscible fluids). An order of magnitude analysis of the entrainment process using this idea was given by Tennekes (11).

3. Analytical development

3.1. Equations and turbulence modelling

Neglecting molecular effects and adopting the Boussinesq approximation, the Reynolds equations for mass and horizontal momentum in the mixed layer may be written

$$\frac{\partial \bar{\rho}}{\partial t} + \frac{\partial}{\partial z} \overline{\rho' w'} = 0 \tag{1a}$$

$$\frac{\partial \bar{u}}{\partial t} + \frac{\partial}{\partial z} \overline{u' w'} = - \frac{1}{\rho_o} \frac{\partial \bar{p}}{\partial x} \tag{1b}$$

where ρ is the density, ρ_o the density of the lower layer, p the pressure, u,w are the horizontal and vertical velocity components, and x,z the horizontal and vertical co-ordinates (the latter is positive in downward direction). Overbars indicate mean values as regards turbulence, and primes indicate fluctuations. The pressure gradient depends on time only. The boundary conditions at the free surface are

$$\overline{\rho'w'} = 0, \qquad z = 0 \tag{2a}$$

$$\overline{u'w'} = u_*^2, \qquad z = 0 \tag{2b}$$

where u_* is the friction velocity. For the time being, the lower layer is assumed to be quiescent (implying neglect of viscous effects)*. Mass transport and shear stress then vanish at, or just below, the interface. This yields the boundary conditions

$$\overline{\rho'w'} = 0, \qquad z = h \tag{3a}$$

$$\overline{u'w'} = 0, \qquad z = h \tag{3b}$$

$$\bar{\rho} = \rho_o, \qquad z = h \tag{3c}$$

$$\bar{u} = 0, \qquad z = h \tag{3d}$$

The integral balances of mass and momentum are

$$\int_0^h (\rho_o - \bar{\rho})\, dz = \Delta\rho_o h_o \tag{4a}$$

$$\frac{\partial}{\partial t} \int_0^h \bar{u}\, dz = u_*^2 - \frac{h}{\rho_o} \frac{\partial \bar{p}}{\partial x} \tag{4b}$$

where $\Delta\rho_o$ is the initial density difference and h_o the initial depth of the upper layer.

The initial, highly unsteady phase after the shear stress has started to act on the free surface is not considered. Only the quasi-steady

* Viscous effects are considered in section 4 to predict the mean horizontal velocit

development of the mixing layer occurring afterwards is examined, see section 3.2.

To make further progress possible, a form of turbulence modelling is required. One of the simpler models starts from the gradient-transport hypothesis,

$$\overline{\rho' w'} \approx - K_s(z,t,Ri) \frac{\partial \bar{\rho}}{\partial z} \tag{5a}$$

$$\overline{u' w'} \approx - K_m(z,t,Ri) \frac{\partial \bar{u}}{\partial z} \tag{5b}$$

Here K_s and K_m are eddy diffusivity and eddy viscosity depending on stability, characterized by the gradient Richardson number Ri,

$$Ri = \frac{g}{\rho_o} \frac{\frac{\partial \bar{\rho}}{\partial z}}{(\frac{\partial \bar{u}}{\partial z})^2} \tag{6}$$

K_s and K_m can be related to the turbulent kinetic energy, $k = \frac{1}{2}(\overline{u'^2} + \overline{v'^2} + \overline{w'^2})$, and the length scale, l, of the large eddies according to the Prandtl-Kolmogorov relations,

$$K_s = c_s \sqrt{k} l$$

$$K_m = c_m \sqrt{k} l$$

where c_s, c_m are coefficients. Some qualitative conclusions regarding the state of the turbulence can be drawn from the transport equation for the kinetic energy. A modelled form of this equation may be written (e.g. 13, 14), for the case under consideration,

$$\frac{\partial k}{\partial t} = \frac{\partial}{\partial z} (\frac{K_m}{\sigma_k} \frac{\partial k}{\partial z}) - \overline{u'w'} \frac{\partial \bar{u}}{\partial z} (1 - Rf) - c_D \frac{k^{3/2}}{l} \tag{7}$$

where σ_k, c_D are coefficients, and Rf is the flux Richardson number defined by

$$Rf = \frac{g\,\overline{\rho' w'}}{\rho_o\,\overline{u'w'}\,\frac{\partial \bar{u}}{\partial z}} = \frac{K_s}{K_m}\,Ri \qquad (8)$$

The terms on the RHS of (7) represent diffusion, production (Rf accounting for buoyancy effects) and dissipation of k, respectively. Rf is found experimentally to be significantly smaller than unity, even under very stable conditions. Since furthermore the coefficients in (7) are of order unity, the orders of magnitude in the central region ($z \sim \frac{1}{2}h$) of the three terms on the RHS are ($\partial\bar{u}/\partial z$ is eliminated using (4b))

$$K_m \frac{k}{h^2}, \quad \frac{(\overline{u'w'})^2}{K_m} \quad \text{and} \quad \frac{k^{3/2}}{l}$$

or, since $K_m \sim \sqrt{k}l$,

$$(\frac{l}{h})^2 \frac{k^{3/2}}{l}, \quad (\frac{\overline{u'w'}}{k})^2 \frac{k^{3/2}}{l} \quad \text{and} \quad \frac{k^{3/2}}{l}$$

If $\overline{u'w'}$ were much less than k, the dissipation term in (7) would be dominant (presumably, diffusion is of secondary importance in many cases*, since $(l/h)^2 << 1$ even under neutral conditions) and turbulence would disappear. A condition for the turbulence to be quasi-stationary therefore is

$$\frac{\overline{u'w'}}{k} \sim (\frac{\overline{u'w'}}{k})_n \qquad (9)$$

Here the subscript n refers to neutral conditions. In near-wall turbulence the ratio $\overline{u'w'}/k$ is known to vary only slightly with stability (e.g. 15), whereas it markedly decreases with increasing stability in free shear flows (e.g. 16, 17). Wall effects depend on the ratio of the size of the large eddies and the distance to the wall (here the free surface and the interface), or, in the present case, on the ratio l/h (18, 14). Under neutral conditions $l/h \sim 0.1$ and wall effects are

* An exception is the case where the vertical velocity gradient becomes zero somewhere within the mixed layer, see also the comment at the end of this section

important throughout the flow. Under very stable conditions l/h would become much less, since l decreases with increasing stability (19), and the turbulence at $z \sim \frac{1}{2}h$ would be of the same character as that in a free shear flow. However, (9) precludes this situation, since $\overline{u'w'}/k$ would then become much less than its value under neutral conditions. It may therefore be concluded that the mixed layer can be only weakly stratified. This conclusion will be seen to be essential for the existence of an upper bound to the entrainment rate. It seems to be in agreement with experimental evidence. Kato and Phillips (4) in their experiments with zero pressure gradient observed velocity profiles which were very much like those in unstratified Couette flow. Long (2) reconsidered Kato and Phillips' experiment and correctly predicted the velocity of the annular screen driving the flow without taking into account any buoyancy effects. Wu (22) did experiments with a zero net horizontal mass transport (implying a longitudinal pressure gradient) and observed velocity profiles similar to those in unstratified flow over a fixed bottom. Furthermore, Tennekes (11) shows that a bulk Richardson number is of the order of the ratio of u_* and the velocity of the screen in Kato and Phillips' experiment, which ratio is experimentally found to be quite small (see also section 4).

In view of the preceding remarks expressions for K_s and K_m sometimes assumed for turbulent Couette flow and channel flow are introduced. Support to this approach is also lent by the study of Csanady (26), who investigates the correspondence between the turbulent flow along a sharp interface (or free surface) and that along a solid wall. A remarkable analogy is found, although the determination of the 'roughness length' of the interface (free surface) is troublesome.

The influence of buoyancy is accounted for by multiplying K_s and K_m with functions, F_s and F_m, of the gradient Richardson number Ri. These considerations lead to the following expressions

$$K_s = \kappa_s u_* z (1 - \frac{z}{h}) F_s(Ri) \tag{10a}$$

$$K_m = \kappa u_* z (1 - \frac{z}{h}) F_m(Ri) \tag{10b}$$

where κ is von Kármán's constant, and κ/κ_s the turbulent Prandtl number under neutral conditions. The influence of the pressure gradient on the turbulence is ignored in equations 10. This restricts the applicability of the present model to relatively weak pressure gradients ($\partial\bar{p}/\partial x \sim \rho_o u_*^2/h$ or less). F_s and F_m are decreasing functions of Ri, and $F_s(0) = F_m(0) = 1$. According to the preceding discussion Ri should be small, so that $F_s \sim F_m \sim 1$.

It is explained in the Appendix that the interface is able to move downwards despite the fact that the eddy diffusivity and the transport of mass vanish at the interface.

As an alternative to (10) the mixing-length hypothesis could be used. The results thus obtained would not differ substantially from those derived here.

Obviously, both models break down when the vertical velocity gradient becomes zero within the mixed layer. A finite value of Ri would then require also a zero gradient of the density, so that both momentum and buoyancy transport would be completely inhibited at this level. This restriction sets an upper bound to the longitudinal pressure gradient that can be dealt with in this way. The interesting case of a zero net horizontal mass-transport, for instance, is just outside the range of applicability of the simple turbulence model adopted.

3.2. Similarity

The equations in section 3.1. permit a similarity solution, which may be written

$$\bar{\rho} = \rho_o - \frac{\Delta\rho_o h_o}{h(t)} P(\eta) \tag{11a}$$

$$\bar{u} = \sqrt{\frac{\Delta\rho_o}{\rho_o} g h_o}\; U(\eta) \tag{11b}$$

$$\eta = \frac{z}{h(t)} \tag{11c}$$

$$h(t) = h_o + w_e t \tag{11d}$$

where P and U are dimensionless density difference and dimensionless velocity, and w_e the unknown but constant entrainment velocity. A constant entrainment velocity also follows from dimensional considerations (20). Substituting (11) into (1) and using boundary conditions (2), (3a) and (3b) yields upon integration for the turbulent transports

$$\overline{\rho' w'} = - w_e \frac{\Delta\rho_o h_o}{h(t)} \eta P(\eta) \tag{12a}$$

$$\overline{u'w'} = (1 - \gamma\eta)\, u_*^2 + w_e \sqrt{\frac{\Delta\rho_o}{\rho_o} gh_o} \int_0^\eta \eta_1 U'(\eta_1) d\eta_1 \tag{12b}$$

where $U' = dU/d\eta$, and γ the (constant) dimensionless pressure gradient,

$$\gamma = \frac{h(t)}{\rho_o u_*^2} \frac{\partial \bar{p}}{\partial x}$$

The remark following (10) as regards the range of pressure gradients considered requires γ to be of order one or less. The integral balances (4) yield the conditions

$$\int_0^1 P(\eta)\, d\eta = 1 \tag{13a}$$

$$\int_0^1 U(\eta)\, d\eta = \frac{1-\gamma}{E\sqrt{Ri_*}} \tag{13b}$$

where $E = w_e/u_*$, and $Ri_* = \Delta\rho_o\, g\, h_o/(\rho_o u_*^2)$ is an overall Richardson number. The boundary conditions (3c) and (3d) give $P(1) = U(1) = 0$. Equations 12 then show, for $\eta = 1$, that the conditions (3a) en (3b) are consistent with the conditions (3c) and (3d). Integrating (12b) by parts and substituting $\eta = 1$ then again yields (13b). The latter equation shows that a zero net horizontal mass-transport corresponds with a value of γ equal to unity. Equation 13b therefore gives as a necessary condition that γ should be less than unity for the velocity gradient not to become zero. Equation 6 becomes

$$Ri = \frac{-P'}{(U')^2} \tag{14}$$

Introducing the expressions for the turbulent transports, equations 5 and 10, (12) becomes

$$EP + \kappa_s(1-\eta)\; P'\; F_s \left[\frac{-P'}{(U')^2}\right] = 0 \tag{15a}$$

$$E \int_0^{\eta} \eta_1 U'(\eta_1)\, d\eta_1 + \kappa\, \eta(1-\eta)\, U'\, F_m \left[\frac{-P'}{(U')^2}\right] + \frac{1-\gamma\eta}{\sqrt{Ri_*}} = 0 \qquad (15b)$$

Equations 15 form a coupled system of non-linear equations with dependent variables P and U'; the only additional condition is given by (13a).

3.3. Solution for small Ri_*

At sufficiently small values of Ri_* buoyancy effects can be anticipated to be irrelevant, which indicates the functions F_s and F_m in (15) to be nearly unity in this case. It is assumed here that $F_s = F_m = 1$, and the conditions for the gradient Richardson number to be small at all depths are determined afterwards. Using (13a), the solution of (15) then becomes

$$P = \left(1 + \frac{E}{\kappa_s}\right)(1-\eta)^{\frac{E}{\kappa_s}} \qquad (16a)$$

$$U' = -\frac{1}{\eta\sqrt{Ri_*}} \left[\left(\frac{1}{\kappa} - \frac{\gamma}{\kappa - E}\right)(1-\eta)^{-1+\frac{E}{\kappa}} + \frac{\gamma}{\kappa - E}\right] \qquad (16b)$$

It is shown below that the exponent in (16b) is always negative. This equation therefore yields as a condition for the vertical velocity-gradient not to become zero

$$\frac{1}{\kappa} - \frac{\gamma}{\kappa - E} > 0$$

or

$$\gamma < 1 - \frac{E}{\kappa} \qquad (17)$$

Equations 14 and 16 give for the gradient Richardson number

$$Ri = ERi_{*} \left(1 + \frac{E}{\kappa_s}\right) \frac{1}{\kappa_s} \frac{\eta^2 (1-\eta)^{1-2\frac{E}{\kappa}+\frac{E}{\kappa_s}}}{\left[\frac{1}{\kappa} - \frac{\gamma}{\kappa - E} + \frac{\gamma}{\kappa - E}(1-\eta)^{1-\frac{E}{\kappa}}\right]^2} \tag{18}$$

Ri will be small at $\eta \simeq 1$, provided

$$1 - 2\frac{E}{\kappa} + \frac{E}{\kappa_s} > 0$$

or

$$E < \frac{\kappa}{2 - \frac{\kappa}{\kappa_s}} \tag{19}$$

Otherwise, Ri would become very large near the interface, and the turbulence would dissappear. Therefore, (19) sets an upper limit to the entrainment rate under nearly neutral conditions. Assuming $\kappa = 0.40$ and $\kappa_s/\kappa = 1.4$ (1, p. 160) yields $E < 0.31$. The actual maximum entrainment rate seems to be $E \simeq 0.28$ (21). Thus Ri is found to tend to zero, or possibly a small positive value, at the interface. This also holds near the free surface.

Equation 18 indicates that, for values of γ well below the upper bound given by (17), buoyancy effects will be negligible at all depths if $ERi_{*} \ll 1$. Those effects do become appreciable, however, if

$$E \sim \frac{1}{Ri_{*}} \tag{20}$$

Since Ri then is of order one in the central region. Equation 20 indicates another upper bound to the entrainment rate, since the flow in the mixed layer can be only weakly stratified.

3.4. Solution for large Ri_{*}

The entrainment rate can be expected to be small, $E \ll 1$, at large values of Ri_{*} (the dimensionless pressure gradient γ is assumed to be of order unity, as before). Therefore, an asymptotic solution of (15) for E tending to zero is sought. Taking for the time being F_s as a function of η rather than of Ri, (15a) may be integrated to give

$$P = C \exp \left[- \frac{E}{\kappa_s} \int_0^{\eta} \frac{d\eta_1}{F_s(\eta_1)(1-\eta_1)} \right] \tag{21}$$

Expanding the exponential function gives

$$P = C \left[1 - \frac{E}{\kappa_s} \int_0^{\eta} \frac{d\eta_1}{F_s(\eta_1)(1-\eta_1)} \right] + O(E^2) \quad \text{if} \quad \ln(1-\eta) = O(1)$$

The (weak) restriction on η, which follows from (21) since $F_s \sim 1$, indicates that a relatively small region near the interface ($\eta = 1$) is excluded. The integration constant C follows from (13a). After some algebra this gives

$$P = 1 + \frac{E}{\kappa_s} \left[\int_0^{1} \frac{d\eta}{F_s(\eta)} - \int_0^{\eta} \frac{d\eta_1}{F_s(\eta_1)(1-\eta_1)} \right] + O(E^2) \quad \text{if } \ln(1-\eta) = O(1) \tag{22}$$

As a result (15a) becomes, with the same restriction on η,

$$E + \kappa_s (1-\eta)\, P'\, F_s\,(Ri) = O(E^2)$$

or, using (14),

$$E - \kappa_s\, (1-\eta)(U')^2\, Ri\, F_s\,(Ri) = O(E^2) \tag{23}$$

The first term in (15b) is small, that is

$$\kappa\, \eta(1-\eta)\, U'\, F_m\,(Ri) + \frac{1-\gamma\eta}{\sqrt{Ri_*}} = \frac{1}{\sqrt{Ri_*}}\, O(E) \quad \text{if} \quad \ln(1-\eta) = O(1) \tag{24}$$

Eliminating U' between (23) and (24) yields

$$E - \frac{\kappa_s}{\kappa^2} \frac{(1-\gamma\eta)^2}{\eta^2(1-\eta)} \frac{1}{Ri_*} \left[1 + O(E) \right] \frac{Ri\, F_s\,(Ri)}{F_m^2(Ri)} = O(E^2)$$

or, substituting from (8)

$$E - \frac{(1-\gamma\eta)^2}{\kappa\eta^2(1-\eta)} \frac{Rf(Ri)}{F_m(Ri)} \frac{1}{Ri_*} = O(E^2) \tag{25}$$

Equation 25 gives Ri as a function of η, so that the function F_s in (22) may be conceived of as a function of η indeed. Equations 22, 24 and 25 represent the first-order solution of (15) in implicit form (a local expansion would be needed near $\eta = 1$).

According to (25), Rf/F_m (and hence Ri) attain a maximum at $\eta = \eta_e$ following from

$$\gamma\eta_e^2 - 3\eta_e + 2 = 0, \qquad \gamma < 1$$

Equation 25 then gives, cf. (20),

$$E \simeq \frac{f(\gamma)}{\kappa} \left(\frac{Rf}{F_m}\right)_{max} \frac{1}{Ri_*} \tag{26}$$

where

$$f(\gamma) = \frac{(1-\gamma\eta_e)^2}{\eta_e^2(1-\eta_e)}$$

Equation 26 shows that, at large Ri_*, the entrainment rate is inversely proportional to Ri_*. This result has been obtained here without introducing the usual assumption that the increase in potential energy is proportional to the work done by the shear stress at the free surface (in the case where $\gamma = 0$).

Figure 2 shows η_e and the factor f in (26) as functions of the dimensionless pressure gradient γ. The turbulence parameter $(Rf/F_m)_{max}$ depends on stability, which, according to the discussion in section 3.1., should be weak. It is therefore reasonable to assume that in first approximation $(Rf/F_m)_{max}$ is independent of γ. The function f then also represents the dependence of the entrainment rate on the pressure gradient (at fixed Ri_*). In the case of zero net horizontal mass-transport γ is equal to unity, see the comment following (13). Figure 2 shows

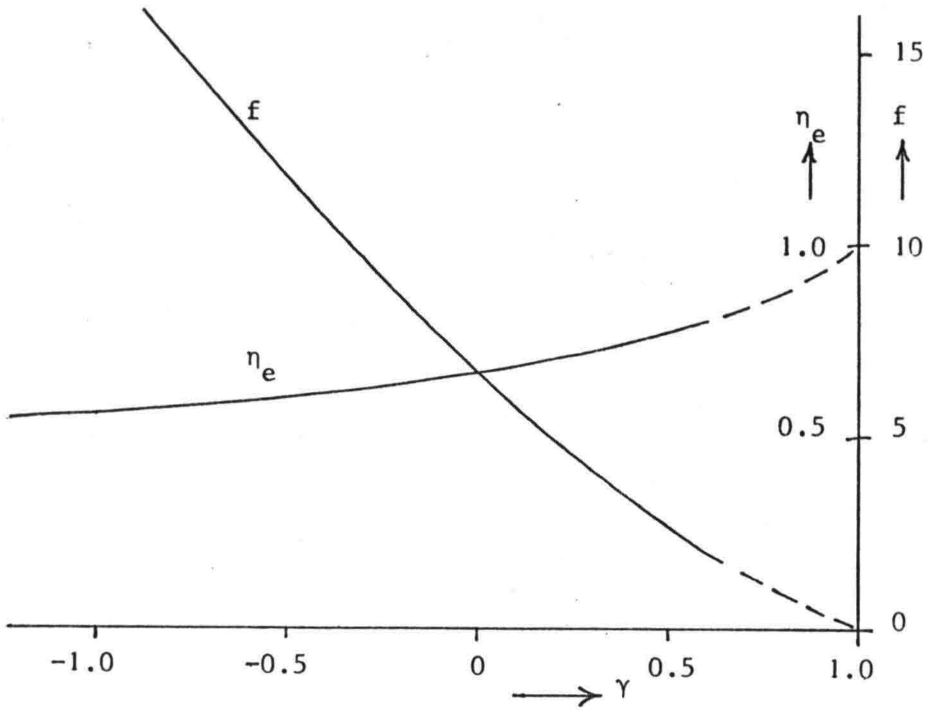

Figure 2. Influence of pressure gradient on entrainment

that the entrainment rate would then be reduced to zero. This result is not reliable, however, since the turbulence model adopted is valid for values of γ (appreciably) less than unity. Nevertheless, the tentative conclusion of a drastically reduced entrainment rate at zero net horizontal mass-transport is in qualitative agreement with the experiments of Wu (22). His results indicate entrainment rates less than 10 per cent of those found by Kato and Phillips ($\gamma = 0$).

The condition of weak stratification implies that the value of the flux Richardson number in the parameter $(Rf/F_m)_{max}$ should be less than its critical value, Rf_{cr}, under very stable conditions. Arya (15) and others (e.g. 1) find $Rf_{cr} \simeq 0.15$ to 0.40. Adopting, as an example, $Rf = 0.1$ (this value is supported by the field measurements of Kullenberg (6)) and $F_m = 0.8$ yields, in the case of a zero pressure gradient, $E \simeq 2/Ri_*$. Obviously, other values of the proportionality constant can be obtained by varying the parameters. The example is not unrealistic, however, and yields entrainment rates in the same order of magnitude as those found experimentally (Kato and Phillips obtained $E \simeq 2.5/Ri_*$).

3.5. A simple model involving a maximum entrainment rate

The discussion in section 3.1. leading to the conclusion of weak stratification was needed to show that the value of F_m in (26) should not differ too much from unity. The model equations underlying (26) do not imply any restrictions as regards the value of F_m.

However, such functions $F_s(Ri)$ and $F_m(R_i)$ can be devised, that the equations mentioned automatically set lower bounds to F_s and F_m. This can be realized by requiring that the parameter

$$\frac{Rf(Ri)}{F_m(Ri)}$$

occurring in (25) and (26) attains a maximum for some (small) value of Ri. As an example consider the linear functions

$$F_s = 1 - \alpha_s Ri \ , \quad Ri < \frac{1}{\alpha_s} \tag{27a}$$

$$F_m = 1 - \alpha_m Ri \ , \tag{27b}$$

where α_s and α_m are constants. Since in the case considered buoyancy transport is more effectively inhibited by stratification than momentum transport (1, p. 160), the coefficient α_m should be smaller than α_s. Equations 27 give (figure 3)

$$\left(\frac{Rf}{F_m}\right)_{max} = \frac{\kappa_s}{\kappa}\,\frac{1}{4(\alpha_s - \alpha_m)} \qquad \text{at} \qquad Ri = \frac{1}{2\alpha_s - \alpha_m} \tag{28a,b}$$

Only Richardson numbers in the range $0 \leqq Ri \leqq 1/(2\alpha_s - \alpha_m)$ are of interest. Equation 28b and figure 3 show that the condition of weak stratification requires the coefficients α_m to be taken much smaller than α_s. The factor $1/(\alpha_s - \alpha_m)$ in (28a) is therefore of the order of magnitude of a critical gradient Richardson number at which turbulence would be completely suppressed. Denoting this parameter by Ri_{cr},

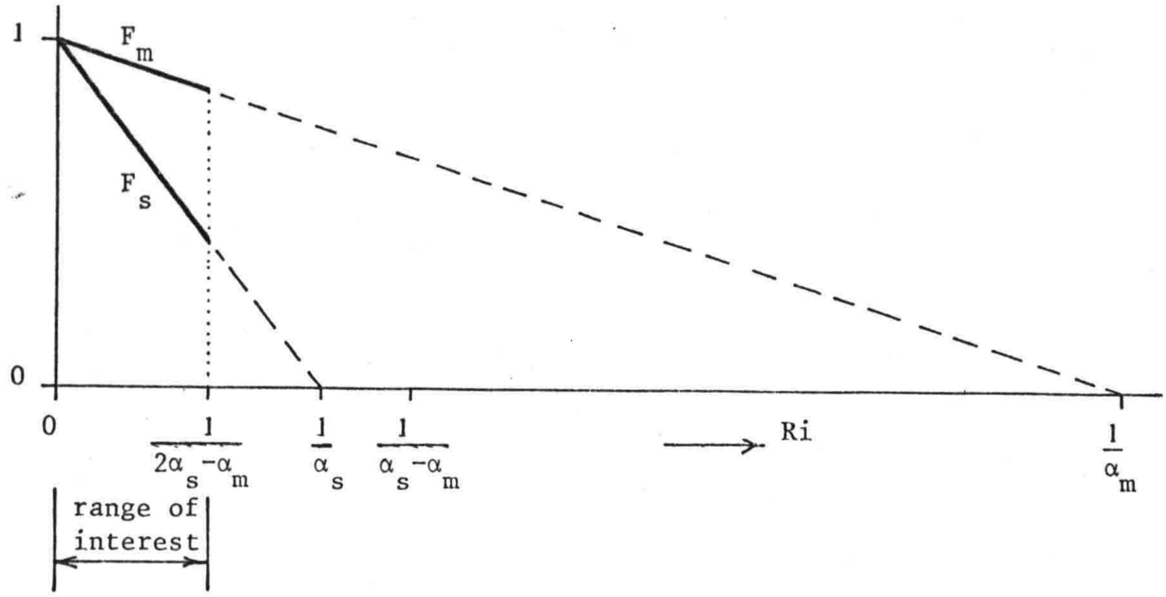

Figure 3. Linear functions F_s and F_m

(26) becomes on substitution from (28a)

$$E \simeq f(\gamma) \frac{\kappa_s}{4\kappa^2} \frac{Ri_{cr}}{Ri_*} \tag{29}$$

Assuming $\kappa_s/\kappa = 1.4$ and, rather arbitrarily, $Ri_{cr} = 0.6$ yields, in the case of a zero pressure gradient, $E \simeq 3.5/Ri_*$, which is again of the same order as experimental values.

4. Estimate of mean velocity at large Ri_*

The theory developed in section 3 aimed at determining the entrainment rate. In the case of large overall Richardson number Ri_*, however, the theory is not adequate to predict the mean velocity in the mixed layer. This can be seen in the following way. The integral balance of momentum, equation 4b, gives together with the similarity assumption (equations 11)

$$w_e \bar{\bar{u}} = u_*^2 - \frac{h}{\rho_o} \frac{\partial \bar{p}}{\partial x} \tag{30}$$

where $\overline{\overline{u}}$ is the mean horizontal velocity,

$$\overline{\overline{u}} = \frac{1}{h} \int_0^h \overline{u}\, dz$$

Substituting from (26) then yields

$$\overline{\overline{u}} \propto \frac{1-\gamma}{u_*}$$

indicating that the mean velocity would tend to infinity, if the friction velocity u_* goes to zero. This physically unrealistic behaviour can be remedied by assuming that the lower layer is able to vertically transfer horizontal momentum. This requires a non-zero (molecular or effective) viscosity of the fluid in this layer. It will be demonstrated that this modification of the theory limits the mean velocity, but practically leaves the entrainment rate unchanged.

A somewhat simplified problem is considered for convenience: buoyancy effects are ignored, that is, the functions F_s and F_m are equated to unity (an overall effect of buoyancy could be absorbed in the coefficients κ_s and κ), and a zero pressure gradient is assumed ($\gamma = 0$).

The flow in the upper layer will now induce a flow in the lower layer. The boundary conditions at the interface become (mass transport in the lower layer is neglected, as before)

$$\overline{\rho' w'} = 0 \tag{31a}$$

$$\overline{u' w'} = (\overline{u' w'})_o \qquad \text{at } z = h \tag{31b}$$

$$\overline{\rho} = \rho_o \tag{31c}$$

$$\overline{u} = \overline{u}_o \tag{31d}$$

where the subscript o refers to the lower layer. The velocity $\overline{u}_o$ is the horizontal velocity just below the interface. The integral balance of momentum for the mixed layer becomes

$$\frac{\partial}{\partial t} \int_0^h \bar{u}\, dz = w_e \bar{u}_o + u_*^2 - (\overline{u'w'})_{z=h}$$

or

$$w_e \, \Delta u = u_*^2 - (\overline{u'w'})_{z=h} \tag{32}$$

where $\Delta u = \bar{\bar{u}} - \bar{u}_o$. The expression for the eddy viscosity in the mixed layer is modified according to

$$K_m = \kappa u_* z \left(1 - \alpha \frac{z}{h}\right) \tag{33}$$

there α is a coefficient, $0 < \alpha < 1$, to account for the non-zero viscosity at and below the interface. Obviously, other distributions of K_m could be assumed for this purpose. Assuming continuity of the (eddy) viscosity profile at $z = h$ gives

$$\kappa u_* h \,(1 - \alpha) = \nu_o \tag{34}$$

where ν_o is the viscosity of the lower layer at $z = h$. Equation 34 determines α. Although h and hence α are slowly varying functions of time, α will be treated as a constant. Equation 34 may be written

$$\alpha = 1 - \frac{1}{\kappa Re_*} \tag{35}$$

where $Re_* = u_* h/\nu_o$ is a Reynolds number. The solution of (15b), with the factor $(1 - \eta)$ now replaced by $(1 - \alpha\eta)$, becomes

$$U' = - \frac{1}{\kappa\sqrt{Ri_*}\; \eta(1 - \alpha\eta)^{1 - \frac{E}{\alpha\kappa}}}$$

from which

$$(\overline{u'w'})_{z=h} = u_*^2 \,(1 - \alpha)^{\frac{E}{\alpha\kappa}} \tag{36}$$

In the case of large Reynolds numbers, (32), (36) and (35) yield for the velocity difference Δu

$$\frac{\Delta u}{u_*} = \frac{1 - (\kappa Re_*)^{-\frac{E}{\kappa}}}{E} \tag{37}$$

For small entrainment rates ($E << \kappa$), consequently for large Ri_*, (37) may be approximated by

$$\frac{\Delta u}{u_*} \approx \frac{1}{\kappa} \ln (\kappa \, Re_*) \tag{38}$$

which shows Δu to remain finite, even if $E = w_e/u_*$ tends to zero, because of the non-zero viscosity of the lower layer. Also, Δu does not depend on Ri_* for large values of this parameter.

The maximum value of Re_* in the experiments of Kato and Phillips (4), and Kantha et al. (20) was about 3000. Equation 38 then gives $\Delta u/u_* < 18$. The dependence on Re_* is weak: $Re_* = 500$ would give $\Delta u/u_* \approx 13$. Kato and Phillips report that in their experiments the horizontal velocity in the central region was about half of that of the screen. Neglecting the velocity in the lower layer, this suggests the relationship

$$\frac{u_s}{u_*} \approx 2 \frac{\Delta u}{u_*} \approx \frac{2}{\kappa} \ln (\kappa \, Re_*) \tag{39}$$

where u_s is the screen velocity. The measured screen velocities were less than those predicted by (39), possibly as a result of side-wall friction. Long (2) derived in a different way

$$\frac{u_s}{u_*} = \frac{2}{\kappa} \ln \frac{h}{a} + A \tag{40}$$

where a and A are unknown constants. Equation 39 gives the same functional dependence of u_s on h, Re_* being proportional to h. Equation 40 can be brought into line with the experimental data of Kato and Phillips, but not with those of Kantha et al.

The influence of the viscosity of the lower layer on the entrainment rate at large Ri_* can be determined in the way described in section 3.4. For large Reynolds numbers, which are relevant from a practical point of view, the equivalent of (26) is

$$E \simeq \left(1 - \frac{4}{\kappa\, Re_*}\right) \frac{27}{4\kappa} (Rf)_{max} \frac{1}{Ri_*} \qquad (41)$$

The function F_m does not appear, since it was equated to unity beforehand. Equation 41 shows that at large Re_* the influence of viscosity on the rate of entrainment is negligibly small, as opposed to the influence on the mean velocity.

5. Concluding remarks

The results obtained indicate that, for the turbulence to be maintained, the stratification can be only weakly stabilized by buoyancy effects, and that this sets an upper bound to the entrainment rate. The relatively good agreement between (26) or (29) and most of the available experimental data (1, 3, 4, 5, 6, the Ri_*^{-1} dependence in (26) and (29) is also found in 7 and 22) suggests the diffusive properties of the mixed layer to control the rate of entrainment indeed. The entrainment process at the interface itself seems not to be the limiting factor.

The experiments of Kantha et al. (20) do not show the Ri_*^{-1} dependence. At large Ri_* the rate of entrainment is found to decrease more rapidly with increasing Ri_*. The explanation of this different behaviour is not clear.

A turbulence model predicting quantitatively correct entrainment rates should account for the decrease in the ratio $\overline{u'w'}/k$ with increasing stability to warrant the mixed layer to remain weakly stratified. The simplest model including this property seems to be an 'algebraic-stress model' (17, 23, 14). In turbulence models of this type the transport equations of the Reynolds stresses are modelled (and drastically simplified) in addition to those for turbulent kinetic energy and dissipation. Turbulence models were applied to wind mixing by Spalding and Svensson (24), and Lewellen et al. (25). These authors report only qualitative agreement with the measurements of Kato and Phillips, however. Possibly, part of the discrepancy is caused by wall effects (here the presence of interface and free surface).

A much simpler, although somewhat artificial and less universal, way to obtain a finite entrainment rate is to prescribe such functions F_s and F_m, that the parameter Rf/F_m attains a maximum at a relatively small value of Ri. In view of the various uncertainties involved, however, turbulence measurements in the mixed layer are indispensable for quantitative predictions.

References

1. Turner, J.S., Buoyancy Effects in Fluids, Cambridge University Press, 1973.
2. Long, R.R., J. Fluid Mech., 70, 2, 1975, pp. 305-320.
3. Sherman, F.S., Imberger, J. and Corcos, G.M., Ann. Rev. Fluid Mech., 10, 1978, pp. 267-288.
4. Kato, H. and Phillips, O.M., J. Fluid Mech., 37, 4, 1969, pp. 643-655.
5. Ottesen Hansen N.-E., J. Hydr. Div., Proc. ASCE, 101, HY8, 1975, pp. 1037-1052.
6. Kullenberg, G., Est. Coast. Mar. Sci., 5, 1977, pp. 329-338
7. Moore M.J. and Long, R.R., J. Fluid Mech. 49, 4, 1971, pp. 635-655.
8. Thorpe, S.A., J. Fluid Mech., 46, 2, 1971, pp. 299-319.
9. Hazel, Ph., J. Fluid Mech., 51, 1, 1972, pp. 39-62.
10. Wyatt, L.R., J. Fluid Mech., 86, 2, 1978, pp. 293-312.
11. Tennekes, H., Mém. Soc. Roy. Sci. Liège, 6, 6, 1973, pp. 131-139.
12. Pedersen, F.B., In: Progress Report No. 45, Technical University Denmark, Institute of Hydrodynamics and Hydraulic Engineering, 1978, pp. 13-22.
13. Launder, B.E. and Spalding, D.B., Lectures in Mathematical Models of Turbulence, Academic Press, 1972.

14. Rodi, W., Turbulence Models and their Application in Hydraulics, a State of the Art Review, Universität Karlsruhe, Sonderforschungsbereich 80 (to appear).

15. Arya, S.P.S., Quart. J. Roy. Meteorol. Soc., 98, 1972, pp. 264-273.

16. Webster, C.A.G., J. Fluid Mech., 19, 2, 1964, pp. 221-245.

17. Launder, B.E., J. Fluid Mech., 67, 3, 1975, pp. 569-581.

18. Daly, B.J. and Harlow, F.H., Phys. Fluids, 13, 11, 1970, pp. 2634-2649.

19. Monin, A.S. and Yaglom, A.M., Statistical Fluid Mechanics: Mechanics of Turbulence, Vol. 1, Ch. IV, MIT Press, 1971.

20. Kantha, L.H., Phillips, O.M. and Azad, R.S., J. Fluid Mech., 79, 4, 1977, pp. 753-768.

21. Tennekes, H. and Lumley, J.L., A First Course in Turbulence, p. 192, MIT Press, 1972.

22. Wu, J., J. Fluid Mech., 61, 2, 1973, pp. 275-287.

23. Gibson, M.M. and Launder, B.E., J. Heat Transf., Trans. ASME, 98, 1976, pp. 81-87.

24. Spalding, D.B. and Svensson, U., In: Heat Transfer and Turbulent Buoyant Convection (D.B. Spalding and N. Afgan, editors), Vol. 1, pp. 113-122, Hemisphere Publ. Corp. and McGraw-Hill, 1977.

25. Lewellen, W.S., Teske, M.E. and Donaldson C. du P. , J. AIAA, 14, 3, 1976, pp. 382-387.

26. Csanady, G.T., J. Geophys. Res., 83, C5, 1978, pp. 2329-2342.

Appendix - Diffusion-controled fronts

The one-dimensional diffusion equation reads, in the absence of advection,

$$\frac{\partial \Gamma}{\partial t} = \frac{\partial}{\partial z} (K \frac{\partial \Gamma}{\partial z}) \tag{A1}$$

where Γ is a scalar quantity like concentration or temperature. The diffusivity K depends on the properties of the medium dispersing the scalar. Assume that a simple, translatory wave is propagating through the otherwise undisturbed medium, and that the diffusive properties of the medium depend on the distance behind the front of this wave according to

$$K(z,t) = 0, \quad z \geqq ct \tag{A2a}$$

$$K(z,t) = K(ct-z), \quad z < ct \tag{A2b}$$

Here c is the velocity of propagation of the wave; the path of the front in the (z,t)-plane is given by $z = ct$. Equation A1 then allows solutions of the form

$$\Gamma(z,t) = \Gamma(ct-z) \tag{A3}$$

which shows that a wave solution does exist under these circumstances. Letting $ct-z = y$, (A1) changes to

$$\frac{d}{dy} (K \frac{d\Gamma}{dy}) - c \frac{d\Gamma}{dy} = 0$$

which may be integrated once to give

$$K \frac{d\Gamma}{dy} - c\Gamma = \text{constant} \tag{A4}$$

As an example, the solution to (A4) is given for the case where the diffusivity behind the front is proportional to the distance to the front ($K = by$, b and $y > 0$). Using (A2a), it is (figure 4a)

$$\Gamma = \Gamma_o \ , \qquad z \geq ct \tag{A5a}$$

$$\Gamma = \Gamma_o + A(ct - z)^{\frac{c}{b}}, \quad z < ct \tag{A5b}$$

Here Γ_o and A are constants of integration. Note the agreement of (A5b) with (16a).

To determine the propagation velocity c, which is arbitrary at this stage, it would be necessary to introduce a controling mechanism behind the front like that described in section 3, for instance.

It is easily verified that in the example considered the transport $(-K\,\partial\Gamma/\partial z)$ vanishes at $z = ct$, and at first sight it may seem contradictory that nevertheless the front can propagate. However, (A1) expresses that the rate of change of the scalar $(\partial\Gamma/\partial t)$ equals (minus) the gradient of the transport $(\partial/\partial z(K\,\partial\Gamma/\partial z))$, and this quantity differs from zero as $z \uparrow ct$ (it even tends to infinity if $c/b < 1$). Therefore, the front is able to travel into the region with zero diffusivity, see also figure 4b.

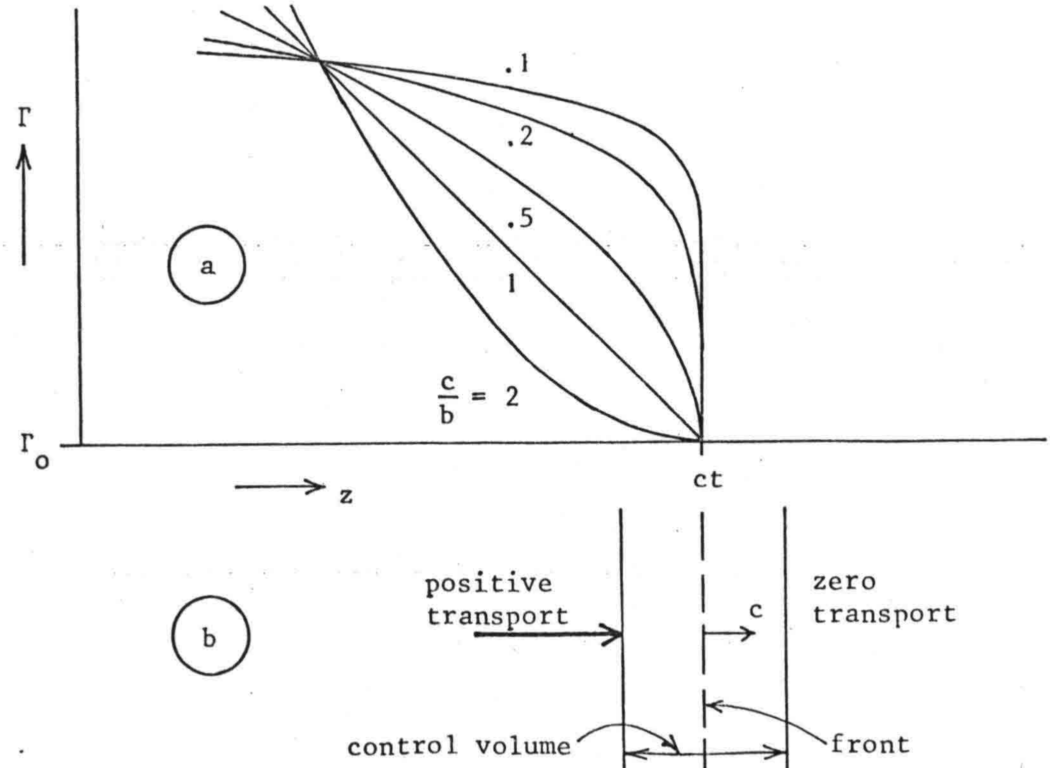

Figure 4. Example of diffusion-controled front, a shape of front for various values of c/b, b control volume enclosing the front